



**HAL**  
open science

## Fossil evidence for serpentinization fluids fueling chemosynthetic assemblages

Franck Lartaud, Crispin T.S. Little, Marc de Rafelis, Germain Bayon, Jerome Dymont, Benoit Ildefonse, Vincent Gressier, Yves Fouquet, Françoise Gaill,  
Nadine Le Bris

► **To cite this version:**

Franck Lartaud, Crispin T.S. Little, Marc de Rafelis, Germain Bayon, Jerome Dymont, et al.. Fossil evidence for serpentinization fluids fueling chemosynthetic assemblages. Proceedings of the National Academy of Sciences of the United States of America, 2011, 108, pp.7698-7703. 10.1073/pnas.1009383108 . insu-01352929

**HAL Id: insu-01352929**

**<https://insu.hal.science/insu-01352929v1>**

Submitted on 10 Aug 2016

**HAL** is a multi-disciplinary open access archive for the deposit and dissemination of scientific research documents, whether they are published or not. The documents may come from teaching and research institutions in France or abroad, or from public or private research centers.

L'archive ouverte pluridisciplinaire **HAL**, est destinée au dépôt et à la diffusion de documents scientifiques de niveau recherche, publiés ou non, émanant des établissements d'enseignement et de recherche français ou étrangers, des laboratoires publics ou privés.

# Fossil evidence for serpentinization fluids fueling chemosynthetic assemblages

Franck Lartaud<sup>a,b,1</sup>, Crispin T. S. Little<sup>c</sup>, Marc de Rafelis<sup>b</sup>, Germain Bayon<sup>d</sup>, Jerome Dymant<sup>e</sup>, Benoit Ildefonse<sup>f</sup>, Vincent Gressier<sup>b</sup>, Yves Fouquet<sup>d</sup>, Françoise Gaill<sup>g</sup>, and Nadine Le Bris<sup>a,h</sup>

<sup>a</sup>Université Pierre et Marie Curie–Paris 6, Laboratoire d'Ecogéochimie des Environnements Benthiques, Centre National de la Recherche Scientifique, Laboratoire Arago, 66650 Banyuls-sur-Mer, France; <sup>b</sup>Université Pierre et Marie Curie–Paris 6, Institut des Sciences de la Terre de Paris, Laboratoire Biominéralisations et Environnements Sédimentaires, Centre National de la Recherche Scientifique 75252 Paris Cedex 05, France; <sup>c</sup>School of Earth and Environment, University of Leeds, Leeds LS2 9JT, United Kingdom; <sup>d</sup>Département Géosciences Marines, Institut Français de Recherche pour l'Exploitation de la Mer, Centre de Brest, 29280 Plouzané, France; <sup>e</sup>Institut de Physique du Globe de Paris, Centre National de la Recherche Scientifique, Equipe Géosciences Marines, 75252 Paris Cedex 05, France; <sup>f</sup>Géosciences Montpellier, Centre National de la Recherche Scientifique, Université Montpellier 2, 34095 Montpellier Cedex 05, France; <sup>g</sup>Centre National de la Recherche Scientifique, Institut Écologie et Environnement, Université Pierre et Marie Curie, Institut de Recherche pour le Développement, Muséum National d'Histoire Naturelle, 75252 Paris Cedex 05, France; and <sup>h</sup>Laboratoire Environnements Profonds, Institut Français de Recherche pour l'Exploitation de la Mer, Centre de Brest, 29280 Plouzané, France

Edited by Norman H. Sleep, Stanford University, Stanford, CA, and approved March 24, 2011 (received for review June 30, 2010)

Among the deep-sea hydrothermal vent sites discovered in the past 30 years, Lost City on the Mid-Atlantic Ridge (MAR) is remarkable both for its alkaline fluids derived from mantle rock serpentinization and the spectacular seafloor carbonate chimneys precipitated from these fluids. Despite high concentrations of reduced chemicals in the fluids, this unique example of a serpentine-hosted hydrothermal system currently lacks chemosynthetic assemblages dominated by large animals typical of high-temperature vent sites. Here we report abundant specimens of chemosymbiotic mussels, associated with gastropods and chemosymbiotic clams, in approximately 100 kyr old Lost City-like carbonates from the MAR close to the Rainbow site (36°N). Our finding shows that serpentinization-related fluids, unaffected by high-temperature hydrothermal circulation, can occur on-axis and are able to sustain high-biomass communities. The widespread occurrence of seafloor ultramafic rocks linked to likely long-range dispersion of vent species therefore offers considerably more ecospace for chemosynthetic fauna in the oceans than previously supposed.

*Bathymodiolus* | Ghost City | ultramafic-hosted | mid-ocean ridge | ecogeochemistry

High-temperature hydrothermal vents occur at very geographically restricted sites in the deep-sea, localized on spreading ridges and arc-related volcanoes. Typically, such vent fluids are metal- and H<sub>2</sub>S-rich and precipitate metallic sulfide chimneys on the seafloor (1, 2). These vents usually support high-biomass invertebrate communities, dominated by a small number of endemic species forming symbioses with diverse chemoautotrophic bacteria (e.g., siboglinid tubeworms, bresiliid shrimp, provaniid gastropods, vesicomysid clams, and bathymodiolin mussels) (1, 3). These symbioses exploit chemical energy from a variety of fluids enriched in reduced compounds, mostly hydrogen sulfide and methane, to fix carbon (4). Along slow and ultraslow spreading ridges, like the Mid-Atlantic Ridge (MAR), ultramafic mantle rocks can be exposed on the seafloor by large offset faults (5). Seawater serpentinization of these peridotites produces hydrogen, which subsequently reacts with CO<sub>2</sub> to form methane (6, 7). Because of this, peridotite-hosted high-temperature vent sites on the MAR (e.g., Rainbow and Logatchev) exhibit elevated levels of methane and hydrogen contents in their fluids. Hydrothermal activity can also occur at off-axis ridge settings. A unique example of this is the Lost City vent field, discovered in the year 2000 on the Atlantis Massif, 30°07'N MAR, at 750- to 850-m depth (8). Here, exothermic serpentinization processes may largely drive the hydrothermal convection, although a contribution of magmatic inputs is not excluded (9). The main difference between this off-axis vent field and the other known vent fields on the MAR-axis is that the majority of the Lost City

vent fluids are metal-poor, low-temperature (40–91 °C), and have high pH (9–11). Further, the Lost City fluids are also highly enriched in H<sub>2</sub> and CH<sub>4</sub> and comparatively lower in H<sub>2</sub>S (10). On contact with ambient seawater these alkaline fluids precipitate chimney structures up to 60 m high composed of carbonates (aragonite and calcite) and brucite (Mg(OH)<sub>2</sub>) (11–13). Sulfide minerals are mostly absent from these chimneys, contrasting strongly with on-axis hydrothermal vent structures (13, 14). The Lost City site has generated considerable interest because this sort of system was likely to have been common in early Earth history and represents a plausible geochemical environment for the emergence of life on this, and potentially other, planets (15, 16).

In the context of the MAR peridotite-hosted vent fields another remarkable feature of Lost City is the lack of typical high-biomass animal assemblages dominated by large chemosynthetic invertebrates: There are currently no *Bathymodiolus* mussel beds or bresiliid shrimp swarms, although the diversity of other invertebrates (particularly small gastropods and polychaete worms) is described as being equivalent to that of high-temperature MAR vent communities (11, 17). Only two living specimens of *Bathymodiolus* aff. *azoricus* have been found at Lost City (18, 19), whereas hundreds of broken shell fragments downslope away from the active chimney areas (19, 20) suggest that the population size might have been much larger in the past and is now almost extinct (19). Dead *B. azoricus* shells have also been recently reported from carbonate chimneys at an inactive site near Lost City (21).

Supporting these observations, the enrichment of reduced compounds in Lost City hydrothermal fluid indicates that these, and similar peridotite-hosted vents, hold the energetic potential to support large aggregations of *Bathymodiolus* mussels, a genus widely distributed along the MAR axis (22). *B. aff. azoricus* at Lost City hosts the same symbiont phylotypes as the methanotrophic and thiotrophic endosymbionts of both *B. azoricus* and *B. puteoserpentis* from on-axis sites on the MAR (18), where the methanotrophic symbiont fixes carbon from methane and the chemolithoautotroph uses sulfide to fix CO<sub>2</sub> (23–25). In addition to methane, DeChaine et al. (18) suggest that *B. aff. azoricus* at Lost City could also be utilizing hydrogen, although hydrogen-oxidizing symbionts have yet to be identified. These authors further

Author contributions: F.L., M.d.R., J.D., B.I., Y.F., F.G., and N.L.B. designed research; F.L., C.T.L., M.d.R., G.B., and V.G. performed research; F.L., C.T.L., M.d.R., G.B., and N.L.B. analyzed data; and F.L., C.T.L., and N.L.B. wrote the paper.

The authors declare no conflict of interest.

This article is a PNAS Direct Submission.

<sup>1</sup>To whom correspondence should be addressed. E-mail: franck.lartaud@obs-banyuls.fr.

This article contains supporting information online at [www.pnas.org/lookup/suppl/doi:10.1073/pnas.1009383108/-DCSupplemental](http://www.pnas.org/lookup/suppl/doi:10.1073/pnas.1009383108/-DCSupplemental).

suggested that hydrogen sulfide would be poorly available for mussels at Lost City (18), based on measured sulfide concentrations from Lost City end-member fluids. However, this hypothesis is not supported by the comparison of the end-member total dissolved sulfide versus temperature ratios between Lost City and the on-axis vent fields (Table S1). The maximum temperature of the habitat of *Bathymodiolus* mussels lies around 15 °C, and it requires significant dilution of the end-member fluids in cold seawater. In this temperature range, the sulfide concentration resulting from the dilution of Lost City end-member fluids should be rather similar to the levels experienced by mussels from on-axis vent fields (22, 26). Recent data (27), moreover, suggest that fluids issuing from flanges on the flanks of Lost City chimneys may indeed have a higher H<sub>2</sub>S/temperature ratio than the end-member fluid. Given the potential availability of these reduced compounds in the Lost City vent fluids for symbionts and free-living chemotrophic microbial populations (28, 29), there is therefore no reason to suppose that Lost City-type fluids should exclude the formation of dense chemosynthetic faunal assemblages.

The findings contained in this paper support the hypothesis that Lost City-type fluids can sustain such communities, while providing further evidence for the suggestions of Kelley et al. (17, 30) that low-temperature hydrothermal circulation on slow-spreading ridges has a widespread distribution. We report previously unreported Lost City-like carbonates containing fossil *Bathymodiolus* shells of large size at high densities, together with smaller numbers of two species of chemosynthetic bivalves and four gastropod species. This fossil assemblage is 110,000 years old (based on radiogenic isotopes) and contains similar species to the *Bathymodiolus* mussel beds from high-temperature vents elsewhere on the MAR. Although geographically close to the Rainbow hydrothermal vent field, the Ghost City carbonates and fossils were clearly associated with a distinct type of environment associated with metal-poor fluid venting, contrasting with all known MAR-axis high-temperature vent fluids. This finding not only reveals the existence of low-temperature hydrothermal circulation in serpentinized systems driving substantial fluxes of reduced chemicals close to the ridge axis, but it also expands the range of marine environments that can support chemosynthetic animal communities.

### Ghost City Carbonates

Eight carbonate blocks were dredged during the MoMAR-DREAM cruise (MoMAR 08 Leg 2, August–September 2008)

from the northwestern flank of the Rainbow massif, which is situated on a nontransform offset at 36°14.15N, 33°53.50W (Fig. 1 and Fig. S1). This site, which we name Ghost City, is 1,200 m northeast of the Rainbow vent field at around 2,100 m water depth. The dredge from which the carbonates were collected sampled a transect around 800 m long on the seafloor and recovered, in addition to the carbonates, three shells of thyasirid bivalves, numerous pieces of serpentinized peridotite, and some troctolites and gabbros. The carbonates are white to ivory in color, ranging from 750 to 25 cm<sup>3</sup> in volume, and most have thin (up to 1 mm) exterior ferric oxyhydroxide (ferrihydrite with Mn component) black crusts upon which solitary corals have grown (Fig. 2A and B and Fig. S2). The carbonate textures range from “layered” (Fig. 2C and Fig. S3), with significant porosity (close to 40%,  $n = 4$ ), to “massive.” This carbonate matrix, which encloses mussel shells with a density of up to 4 shells per 10 cm<sup>3</sup>, lacks metallic oxide or sulfide minerals and consists of varying proportions of authigenic carbonate cements and infilling pelagic calcitic and aragonitic fossils (foraminifera, coccoliths, and a few pteropods; Fig. 2D and Fig. S3). The authigenic carbonate cements consist of aragonite, commonly occurring as radial aggregates of acicular crystals, calcite, and sparser rosettes of glendonite crystals (Fig. 2E and F and Fig. S4). The infilling pelagic sediments have  $\delta^{18}\text{O}$  values of  $3.63 \pm 0.25\text{‰}$  and  $\delta^{13}\text{C}$  values of  $0.93 \pm 0.17\text{‰}$  ( $n = 4$ ). Mixed calcite/aragonite authigenic cements have  $\delta^{18}\text{O}$  and  $\delta^{13}\text{C}$  values of  $4.88 \pm 0.19\text{‰}$  and  $-0.66 \pm 1.18\text{‰}$ , respectively ( $n = 9$ ) (Table 1). The authigenic carbonates and the infilling pelagic sediment show good separation between  $\delta^{13}\text{C}$  and  $\delta^{18}\text{O}$  on a canonical discriminant analysis (CDA) scatterplot, supporting distinct mineralization process (Fig. 3 and Table S2). Isotopic measurements of a series of subsamples from one authigenic carbonate crust gave U/Th ages ranging from  $46 \pm 0.3$  kyr to  $193 \pm 11$  kyr ( $n = 4$ ) (Table 2). These samples, however, display a wide range of initial  $\delta^{234}\text{U}$  values (from approximately 129 to 183‰), suggesting that their U/Th ages may be possibly biased due to postformation interaction with seawater or diagenesis (31). One of these subsamples is characterized by a  $\delta^{234}\text{U}_{\text{initial}}$  value ( $150 \pm 1\text{‰}$ ; Table 2) close to the modern seawater signature ( $146.6 \pm 2.6\text{‰}$ ) (31), which suggests that its U/Th ratio may be considered as the most representative of the formation age of Ghost City carbonates. The corresponding U/Th age ( $110 \pm 0.9$  kyr) lies in the same range as the older chimneys from Lost City ( $122 \pm 12$  kyr) (32) and suggests that

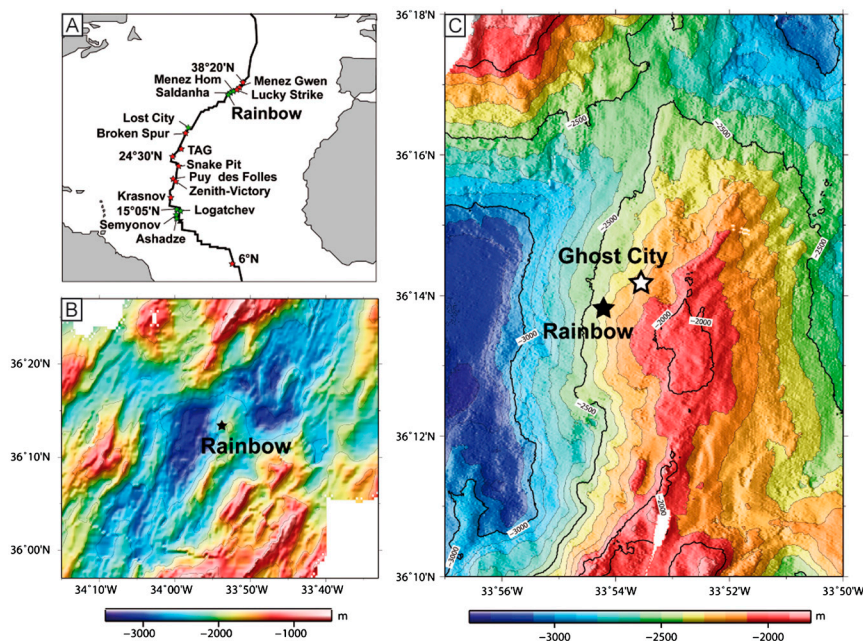


**Fig. 1.** Location of the Ghost City fossil hydrothermal field at different scales. (A) Large scale map showing hydrothermal vents hosted by volcanic rocks (red dots) and gabbros and peridotites (green dots); Ghost City is in the vicinity of the Rainbow hydrothermal field. (B) Standard multibeam bathymetrical map of three MAR segments between 36°00 and 36°20N. These segments show a typical slow-spreading axial valley offset by two nontransform discontinuities. Both Rainbow and Ghost City are located at the northern end of the segment centered on 36°10N. (C) High resolution multibeam bathymetric map acquired at low ship speed during the Flores cruise of the R/V L'Atalante showing the Rainbow vent field on the western flank of the Rainbow massif; the Ghost City fossil site is located on the northwestern flank of this gabbroic and peridotitic structure approximately 1,200 m northeast of the Rainbow vent field, at a depth of 2,100 m.





**Table 2. U-Th ages for Ghost City carbonate samples**

Sample	Corrected U-Th age (kyr) ± 2σ	Initial δ <sup>234</sup> U (‰) ± 2σ
S1	195 ± 11	183 ± 10
S2	110 ± 0.9	150 ± 1
S3	65 ± 11	170 ± 1
S4	46 ± 0.3	129 ± 1

isotopic signature reflect a mixed inorganic carbon source with contributions from seawater ( $\delta^{13}\text{C}_{\text{DIC}} \sim 0\text{‰}$ ) and an isotopically lighter-DIC source. Owing to the very low concentration of inorganic carbon in serpentinization fluids, the most likely origin for this  $^{13}\text{C}$  depleted DIC is the oxidation of methane. Methane in serpentinization fluids are characterized by light carbon isotopic signatures (e.g.,  $\delta^{13}\text{C}_{\text{CH}_4} = -7\text{‰}$  in the Zambales ophiolite,  $-10.3\text{‰}$  at Logatchev,  $-16.7\text{‰}$  at Rainbow, and  $-11.9\text{‰}$  at Lost City) (42–45), which can be further fractionated by methanotrophic microbes converting methane into inorganic carbon. While abiotic methane oxidation is kinetically inhibited at low temperature (46), microbial oxidation of methane can occur in subsurface habitats with various electron acceptors (e.g., oxygen and sulfate) during the mixing of seawater with end-member fluids (47, 48). According to Proskurowski et al. (48), the fractionation factor resulting of anaerobic or aerobic methane oxidation can be as high as 1.039 (49, 50) and will result in further depletion of the initial carbon isotopic ratio by at least  $-13\text{‰}$ . Only a small fraction (approximately 5%) of this  $^{13}\text{C}$  depleted methane is thus sufficient to explain the slightly negative carbon isotopic signature of some Ghost City carbonates. An additional contribution from biogenic methane formed during the subsurface mixing of seawater and the end-member fluid, as described in Proskurowski et al. (48), cannot be ruled out. This assumption is supported by the identification of both methanogenic and anaerobic methane-oxidizing Archaea at Lost City, particularly in the less active chimneys where seawater mixing is occurring (28). In Lost City-type conditions, seawater is the only source of  $\text{HCO}_3^-$ , and mixing is required to compensate the poor supply of this ion from the fluid. As a consequence, the substantial isotopic fractionation resulting of biogenic methane formation that was observed at basalt-hosted diffuse vents (48) may not be achieved due to limiting inorganic carbon conditions. The relative importance of biogenic methane is therefore difficult to estimate from Ghost City samples' isotopic ratios.

The geological context, as well as petrographic and isotopic data, provides supporting evidence that the Ghost City carbonates were formed 110,000 years ago from venting of metal-poor fluids. Despite the proximity with the Rainbow high-temperature vents field, the lack of polymetallic sulfide precipitates in the Ghost City carbonate samples precludes a high-temperature metal-rich hydrothermal fluid contribution in their formation. More likely, these fluids were formed from low-temperature hydrothermal circulation related to serpentinization and were probably close in composition to those currently venting at Lost City.

### Ghost City Fossils

We counted 146 specimens of the mussel *Bathymodiolus* aff. *azoricus* on the exposed surfaces of the eight Ghost City carbonate blocks (Fig. 4 and Fig. S4). The shells range in length from 5 mm to 84 mm, which is comparable to living *B. azoricus* shells from high-temperature hydrothermal vent fields on the MAR (51). Very few of the Ghost City mussel shells are fragmented, and quite a few specimens have articulated valves, with a ratio of 3.6 disarticulated to articulated shells ( $n = 73$ ). Some of the small articulated mussel shells are nested within larger articulated specimens (Fig. 2D). These features are indicative of in situ growth and a lack of post mortem transport. This interpretation is supported by the isotope composition of the Ghost City *B. aff.*

*azoricus* shells ( $\delta^{18}\text{O} = 4.93 \pm 0.40\text{‰}$ ,  $\delta^{13}\text{C} = -0.30 \pm 1.99\text{‰}$ ,  $n = 3$ ; Table 1), values that are more similar to the Ghost City authigenic carbonates than living *Bathymodiolus* shells from the Rainbow high-temperature hydrothermal vent site (CDA analysis; Fig. 3 and Table S2). The other benthic fossils enclosed within the Ghost City carbonate samples (Fig. 4) comprise serpulid tubes ( $>30$ ); the vesicomyid clam *Phreagena* sp. ( $n = 2$ ); the thyasirid clam *Thyasira* sp. ( $n = 1$ ); the limpet *Paralepetopsis* aff. *ferrugivora* ( $n = 15$ ); and the snails *Protolira* aff. *thorvaldssoni* ( $n = 32$ ), *Phymorhynchus* sp. ( $n = 1$ ), *Anatoma* sp. ( $n = 2$ ), and *Lurifax vitreus* ( $n = 1$ ). These also show variable preservation, but in general the shells that were originally aragonitic (the gastropods and clams) show more dissolution and recrystallization than the mixed calcite/aragonite mussel shells, an observation consistent with prolonged seawater interaction (Fig. S5). The Ghost City mollusk assemblage shares five taxa with living MAR axial high-temperature vent communities (3, 52–54), including two locally at Rainbow (*Bathymodiolus* and *Protolira*), and two taxa associated with sedimented vent sites (Table S3). The Ghost City *Phreagena* sp. is also found at the recently described Clamstone site, an inactive (approximately 25 kyr BP) serpentine-hosted sedimented vent field near Rainbow (approximately 1.2 km east of Ghost City, at a depth of 1,980 m) (55). Thyasirid clams that may be conspecific with the Ghost City *Thyasira* sp. occur at Clamstone (55), Anya's Garden, a sedimented vent site in the Logatchev area (52, 56, 57), and have also been reported in

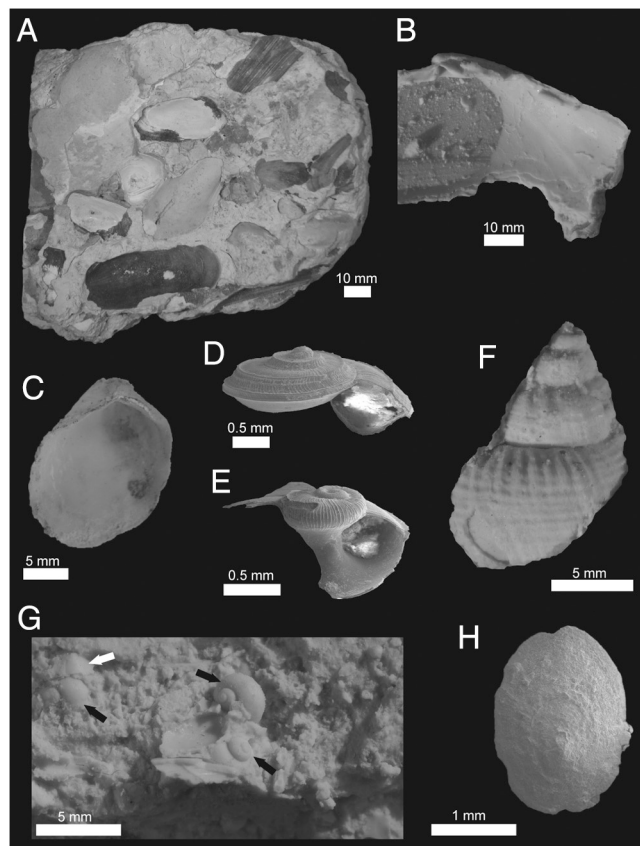


**Fig. 4.** Fossils from Ghost City carbonates. (A) Carbonate block with numerous specimens of *Bathymodiolus* aff. *azoricus*, showing varying degrees of shell preservation. (B) Silicone rubber cast of vesicomyid bivalve *Phreagena*, right valve interior. (C) Thyasirid bivalve, left valve interior. (D) Gastropod *Lurifax vitreus*, oblique apertural view. (E) Gastropod *Anatoma* sp., oblique view of damaged specimen. (F) Silicone rubber cast of gastropod *Phymorhynchus* sp., side view. (G) Silicone rubber cast from carbonate containing three *Protolira* aff. *thorvaldssoni* gastropod specimens (black arrows) and a single limpet (white arrow). (H) Limpet *Paralepetopsis* aff. *ferrugivora*, abapertural view of slightly corroded specimen.



soft sediments at Lost City (20). Thus, the Ghost City mollusk fauna is a mixture of MAR vent species from sedimented sites and more typical chimney habitat mussel bed communities. Although Ghost City fauna has a higher biomass, the mollusk species list is not greatly different from Lost City communities, with three mollusk species shared between the two sites: *B. azoricus*, *Thyasira* species, and the gastropod *Lurifax* (see Table S3).

### High-Biomass Vent Communities Supported by Serpentinization Fluids

The Ghost City carbonates demonstrate that (i) high-biomass populations of *Bathymodiolus* mussels and other symbiont-hosting mollusks can be supported by metal-depleted and likely alkaline fluids, similar to the serpentinization-related vent fluids described at Lost City; and (ii) these communities have been present on the axis of the MAR for at least 110,000 years. The flexible *B. azoricus* dual symbiosis responds to variations in the methane-to-sulfide ratio in the environment (24, 25), making this species particularly well adapted to the variety of fluid chemistries that are found on the MAR (8, 58). The Ghost City fossil mussels might therefore also have relied on methanotrophy and, potentially, on sulfide, or even hydrogen, oxidation as primary energy pathways. Although the geological setting is different, there is evidence that some other *Bathymodiolus* species are able to exploit diverse energy sources present in a serpentinization context. At the South Chamorro serpentinite seamount in the Mariana forearc, mussels thrive in sedimented cracks in seafloor carbonate cement, and based on soft tissue carbon and sulfur isotopic data, Yamanaka et al. (41) suggest that the mussels host both methanotrophic and thiotrophic symbionts, utilizing both methane from serpentinization reactions and sulfur produced by sulfate reducing bacteria in the sediment. Additionally, vesicomids (4, 59) and many of the studied large thyasirid (4, 52) species host sulfide-oxidizing symbionts, and the presence of representative species in the Ghost City carbonates suggests that a threshold amount of sulfide was present in the Ghost City environment.

### Implications

It is unclear why communities of symbiont-hosting mollusks, including high densities of large *Bathymodiolus* mussels, do not currently persist at Lost City, when they have been present in the past as shown by accumulations of dead shells. Because *Bathymodiolus azoricus* is able to exploit variable chemical energy sources, the most likely explanation is to be searched for in the ecological processes that govern community dynamics in fragmented habitats. One possible cause of this extinction may be related to the dispersal potential of vent species. Lost City is located further from the ridge axis than Ghost City and may have lacked of sufficient larval flow from high-temperature Rainbow-like vent field communities after a major disturbance event. Another explanation could be that the focused flow chimney complex at Lost City lacks the mild temperature diffuse flow areas (<15 °C) with substantial concentrations of electron donors like methane or sulfide, that characterize suitable habitat for vent mussels (22). Further investigation of Lost City habitat conditions and population genetics will help discriminating between these hypotheses.

The findings further support the hypothesis of a widespread occurrence of hydrothermal fluid circulation hosted in exposed ultramafic rocks on the ocean floor (60). The estimated duration of serpentinization-related fluid venting (over 10 kyr to 100 kyr time scales) (32) contrasts strongly with the geographically restricted and short-lived high-temperature vent fields known

to date. Our results indicate that exposed mantle rocks undergoing serpentinization could host deep-sea chemosynthetic vent communities in a wide range of geological settings, including slow and ultraslow spreading ridge axes, off-axis Oceanic Core Complexes (61), continental margins (62), and serpentinite seamounts in forearc settings (63). The exploration of ultramafic rock exposures in the deep sea is thus a fertile area for the understanding both long-range larval dispersal of vent species and the specific requirements for settlement and growth of chemosynthetic animals.

### Methods

**XRD Analyses.** Analyses of carbonate matrix, oxide crust, and mussel shells were made at the ITeP laboratory (UPMC Univ Paris 06) on a Siemens D501. *Bathymodiolus* aff. *azoricus* mussel shells were scrubbed in distilled water with a toothbrush immediately upon collection to remove loosely attached biogenic and inorganic particles. Sample powders of original calcitic outer layer and aragonitic inner layer of the shells were drilled from a depth of approximately 0.1 mm.

**Optical Petrography.** Polished thin sections of carbonates were observed using a stereomicroscope Zeiss SteREO Discovery V20 (Fig. 2 and Fig. S1) Porosity measurements were made using JMicrovision software ([www.jmicrovision.com](http://www.jmicrovision.com)).

**Carbon and Oxygen Stable Isotopes Analyses.** Analyses of three *Bathymodiolus* aff. *azoricus* shells and 13 carbonate matrix (authigenic carbonate and infilling pelagic sediments) Ghost City samples were made on a VG Micromass 602 mass spectrometer. Additionally, five shells of living *B. azoricus* from the Rainbow vent field were analyzed. Powdered samples from mussel shells for the isotopic analyses (3–4 mg) were obtained from the cleaned outer layer using a rotary drill with a diamond-tipped burr. The shell sample powders were pretreated with 1.5 % NaClO for 30 min to remove organic contaminants, rinsed three times with distilled water following a protocol modified after (64, 65). All carbonate powders were acidified in 100% phosphoric acid at 50 °C under vacuum. The produced CO<sub>2</sub> was collected and analyzed using the mass spectrometer. Isotopic data are reported in conventional delta (δ) notation relative to the Vienna Pee Dee Belemnite (VPDB). The standard used for the analyses was an internal standard calibrated on the NBS-19. Standard deviation for δ<sup>18</sup>O and δ<sup>13</sup>C is ±0.10‰.

**Uranium/Thorium and Strontium Analyses.** Analyses were made in the Pôle Spectrométrie Océan (Brest) on a Neptune MC-ICPMS. For uranium and thorium isotope measurements, about 2 mg of carbonate sample was dissolved in 7.5M HNO<sub>3</sub> and spiked with a mixed <sup>236</sup>U/<sup>229</sup>Th spike (66). U and Th were separated chemically using conventional anion exchange techniques adapted from previous studies (67). U and Th concentrations and isotope ratios were then measured in the MC-ICPMS. The carbonate age was corrected for detrital contamination (inherited <sup>230</sup>Th) using measured <sup>232</sup>Th concentrations and assuming a typical <sup>232</sup>Th/<sup>230</sup>Th ratio (150,000) for the contaminant detrital phase, but this correction was insignificant on the calculated age (about 1%) (68). Strontium was isolated using Sr resin and the isotope ratios were measured using the MC-ICPMS. Isotope ratios were normalized to <sup>86</sup>Sr/<sup>88</sup>Sr = 0.1194 and corrected from <sup>87</sup>Rb and <sup>86</sup>Kr interferences on the <sup>87</sup>Sr and <sup>86</sup>Sr signal, respectively.

**ACKNOWLEDGMENTS.** We thank captain and crew of R/V L'Atalante; the remotely operated vehicle Victor operation group; the MoMARDREAM scientific party for their support during the MoMARDREAM cruise; E. Rongemaille, N.-C. Chu, and E. Ponzevera for analytical work; E. Krylova for vesicomid and thyasirid bivalve identification; and A. Wären for benthic gastropod identification. T.M. Shank and A.L. Meistertzheim are also thanked for their helpful comments. The manuscript also benefited from helpful comments from G. Proskurovski and one anonymous reviewer. Centre National de la Recherche Scientifique (CNRS)-INSU, CNRS-INEE, IFREMER, and GENAVIR are gratefully acknowledged for their financial and technical support. The study was part of the CHEMECO collaborative project from the ESF EUROCORES EURODEEP and benefited from the joint support of Fondation TOTAL and UPMC to the chair "Extreme environment, biodiversity and global change."

1. Van Dover CL (2000) *The Ecology of Deep-Sea Hydrothermal Vents* (Princeton Univ Press, Princeton).
2. Von Damm KL (1990) Seafloor hydrothermal activity: Black smoker chemistry and chimneys. *Annu Rev Earth Planet Sci* 18:173–204.

3. Desbruyères D, Segonzac M, Bright M (2006) *Handbook of Deep-Sea Hydrothermal Vent Fauna—Mollusca* (Denisia, Linz, Austria), pp 141–172.
4. Dubilier N, Bergin C, Lott C (2008) Symbiotic diversity in marine animals: The art of harnessing chemosynthesis. *Nat Rev Microbiol* 6:725–740.

5. Cannat M (1993) Emplacement of mantle rocks in the seafloor at mid-ocean ridges. *J Geophys Res* 98:4163–4172.
6. Abrajano TA, et al. (1988) Methane-hydrogen gas seeps, Zambales Ophiolite, Philippines: Deep or shallow origin? *Chem Geol* 71:211–222.
7. Berndt ME, Allen DE, Seyfried WE, Jr (1996) Reduction of CO<sub>2</sub> during serpentinization of olivine at 300 °C and 500 bar. *Geology* 24:351–354.
8. Kelley DS, et al. (2001) An off-axis hydrothermal vent field near the Mid-Atlantic Ridge at 30°N. *Nature* 412:145–149.
9. Allen DE, Seyfried WE, Jr (2004) Serpentinization and heat generation: Constraints from Lost City and Rainbow hydrothermal systems. *Geochim Cosmochim Acta* 68:1347–1354.
10. Proskurowski G, Lilley MD, Kelley DS, Olson EJ (2006) Low temperature volatile production at the Lost City Hydrothermal Field, evidence from a hydrogen stable isotope geothermometer. *Chem Geol* 229:331–343.
11. Kelley DS, et al. (2005) A serpentinite-hosted ecosystem: The Lost City hydrothermal field. *Science* 307:1428–1434.
12. Früh-Green GL, et al. (2003) 30,000 years of hydrothermal activity at the Lost City vent field. *Science* 301:495–498.
13. Ludwig KA, Kelley DS, Butterfield DA, Nelson BK, Früh-Green GL (2006) Formation and evolution of carbonate chimneys at the Lost City Hydrothermal Field. *Geochim Cosmochim Acta* 70:3625–3645.
14. Fouquet Y, et al. (1993) Tectonic setting and mineralogical and geochemical zonation in the Snake Pit sulfide deposit (Mid-Atlantic Ridge at 23°N). *Econ Geol* 88:2018–2036.
15. Holm NG, Charlou JL (2001) Initial indications of abiogenic formation of hydrocarbons in the Rainbow ultramafic hydrothermal system, Mid-Atlantic Ridge. *Earth Planet Sci Lett* 191:1–8.
16. Sleep NH, Meibom A, Fridriksson T, Coleman RG, Bird DK (2004) H<sub>2</sub>-rich fluids from serpentinization: Geochemical and biotic implications. *Proc Natl Acad Sci USA* 101:12818–12823.
17. Kelley DS, Früh-Green GL, Karson JA, Ludwig KA (2007) The Lost City hydrothermal field revisited. *Oceanography* 20:90–99.
18. DeChaine EG, Bates AE, Shank TM, Cavanaugh CM (2006) Off-axis symbiosis found: Characterization and biogeography of bacterial symbionts of *Bathymodiolus* mussels from Lost City hydrothermal vents. *Environ Microbiol* 8:1902–1912.
19. Shank TM, Buckman KL, Butterfield D, Kelley D (2006) Macrofaunal characterization of peridotite-hosted ecosystems associated with Lost City hydrothermal field. *Eos Trans AGU* 87(36):OS10–35 Abstract.
20. Gebruk AV, Galkin SV, Krylova EM, Vereshchaka AL, Vinogradov VM (2002) Hydrothermal fauna discovered at Lost City (30°N, Mid-Atlantic Ridge). *InterRidge News* 11:18–19.
21. Dara OM, Kuz'mina TG, Lein AY (2009) Mineral associations of the Lost Village and Lost City hydrothermal fields in the North Atlantic. *Oceanology* 49:688–696.
22. Le Bris N, Duperron S (2010) Chemosynthetic communities and biogeochemical energy pathways along the MAR: The case of *Bathymodiolus azoricus*. *Diversity of Hydrothermal Systems on Slow-Spreading Ocean Ridges*, eds PA Rona, CW Devey, J Dymont, and BJ Murton (American Geophysical Union, Washington, DC), Vol 188, pp 409–429.
23. Fiala-Medioni A, et al. (2002) Ultrastructural, biochemical, and immunological characterization of two populations of the mytilid mussels *Bathymodiolus azoricus* from the Mid-Atlantic Ridge: Evidence for a dual symbiosis. *Mar Biol* 141:1035–1043.
24. Duperron S, et al. (2006) A dual symbiosis shared by two mussel species, *Bathymodiolus azoricus* and *Bathymodiolus puteoserpentis* (Bivalvia: Mytilidae), from hydrothermal vents along the northern Mid-Atlantic Ridge. *Environ Microbiol* 8:1441–1447.
25. Riou V, et al. (2008) Influence of chemosynthetic substrates availability on symbiont densities, carbon assimilation and transfer in the dual symbiotic vent mussel *Bathymodiolus azoricus*. *Biogeosci Discuss* 5:2279–2304.
26. Desbruyères D, et al. (2001) Variations in deep-sea hydrothermal vent communities on the Mid-Atlantic Ridge near the Azores plateau. *Deep Sea Res Part 1* 48:1325–1346.
27. Konn C, et al. (2009) Hydrocarbons and oxidized organic compounds in hydrothermal fluids from Rainbow and Lost City ultramafic-hosted vents. *Chem Geol* 258:299–314.
28. Brazelton WJ, Schrenk MO, Kelley DS, Baross JA (2006) Methane- and sulfur-metabolizing microbial communities dominate the Lost City hydrothermal field ecosystem. *Appl Environ Microbiol* 72:6257–6270.
29. Brazelton WJ, et al. (2010) Archaea and bacteria with surprising microdiversity show shifts in dominance over 1,000-year time scales in hydrothermal chimneys. *Proc Natl Acad Sci USA* 107:1612–1617.
30. Cannat M, Fontaine F, Escartin J (2010) Serpentinization and associated hydrogen and methane fluxes at slow spreading ridges. *Diversity of Hydrothermal Systems on Slow Spreading Ocean Ridges*, eds PA Rona, CW Devey, J Dymont, and BJ Murton (American Geophysical Union, Washington, DC), Vol 188, pp 241–264.
31. Robinson LF, Belshaw NS, Henderson GM (2004) U and Th concentrations and isotope ratios in modern carbonates and waters from the Bahamas. *Geochim Cosmochim Acta* 68:1777–1789.
32. Ludwig KA, et al. (2011) U-Th systematics and <sup>230</sup>Th ages of carbonate chimneys at the Lost City Hydrothermal Field. *Geochim Cosmochim Acta* 75:1869–1888.
33. Kuznetsov K, et al. (2006) <sup>230</sup>Th/U dating of massive sulfides from the Logatchev and Rainbow hydrothermal fields (Mid-Atlantic Ridge). *Geochronometria* 25:51–55.
34. Eickmann B, Bach W, Peckmann J (2009) Authigenesis of carbonate minerals in modern and Devonian ocean-floor hard rock. *J Geol* 117:307–323.
35. Ribeiro Da Costa I, Barriga FJAS, Taylor RN (2008) Late seafloor carbonate precipitation in serpentinites from the Rainbow and Saldanha sites (Mid-Atlantic Ridge). *Eur J Mineral* 20:173–181.
36. Buchardt B, et al. (1997) Submarine columns of ikaite tufa. *Nature* 390:129–130.
37. Selleck BW, Carr PF, Jones BG (2007) A review and synthesis of glendonites (pseudomorphs after ikaite) with new data: assessing applicability as recorders of ancient coldwater conditions. *J Sediment Res* 77:980–991.
38. Mével C (2003) Serpentinization of abyssal peridotites at mid-ocean ridges. *CR Geosci* 335:825–852.
39. Haggerty JA (1991) Evidence from fluid seeps atop serpentine seamounts in the Mariana forearc: Clues for emplacement of the seamounts and their relationship to forearc tectonics. *Mar Geol* 102:293–309.
40. Kato K, Wada H, Fujioka K (1998) Carbon and oxygen isotope composition of carbonate chimney from Mariana forearc seamount. *JAMSTEC Deep Sea Res* 14:213–222.
41. Yamanaka T, et al. (2003) Stable isotope evidence for a putative endosymbiont-based lithotrophic *Bathymodiolus* sp. mussel community atop a serpentine seamount. *Geomicrobiol J* 20:185–197.
42. Abrajano TA, et al. (1990) Geochemistry of reduced gas related to serpentinization of the Zambales ophiolite, Philippines. *Appl Geochem* 5:625–630.
43. Lilley MD, et al. (1993) Anomalous CH<sub>4</sub> and NH<sub>4</sub><sup>+</sup> concentrations at unsedimented mid-ocean-ridge hydrothermal system. *Nature* 364:45–47.
44. Charlou JL, et al. (2010) High production and fluxes of H<sub>2</sub> and CH<sub>4</sub> and evidence of abiogenic hydrocarbon synthesis by serpentinization in ultramafic-hosted hydrothermal systems on the Mid-Atlantic Ridge. *Diversity of Hydrothermal Systems on Slow-Spreading Ocean Ridges*, eds PA Rona, CW Devey, J Dymont, and BJ Murton (American Geophysical Union, Washington, DC), pp 265–296.
45. Proskurowski G, et al. (2008) Abiogenic hydrocarbon production at Lost City hydrothermal field. *Science* 319:604–607.
46. Webley PA, Tester JW (1991) Fundamental kinetics of methane oxidation in supercritical water. *Energy Fuels* 5:411–419.
47. Valentine DL, Reeburgh WS (2000) New perspectives on anaerobic methane oxidation. *Environ Microbiol* 2:477–484.
48. Proskurowski G, Lilley MD, Olson EJ (2008) Stable isotopic evidence in support of active microbial methane cycling in low-temperature diffuse flows vents at 9°50'N East Pacific Rise. *Geochim Cosmochim Acta* 72:2005–2023.
49. Whiticar MJ, Faber E (1986) Methane oxidation in sediment and water column environments— isotopic evidence. *Org Geochem* 10:759–768.
50. Templeton AS, Chu KH, Alvarez-Cohen L, Conrad ME (2006) Variable carbon isotope fractionation expressed by aerobic CH<sub>4</sub>-oxidizing bacteria. *Geochim Cosmochim Acta* 70:1739–1752.
51. Comtet T, Desbruyères D (1998) Population structure and recruitment in mytilid bivalves from the Lucky Strike and Menez Gwen hydrothermal vent fields (37°17'N and 37°50'N on the Mid-Atlantic Ridge). *Mar Ecol Prog Ser* 163:165–177.
52. Southward EC, Gebruk AV, Kennedy H, Southward AJ, Chevaldonné P (2001) Different energy sources for three symbiont-dependent bivalve mollusks at the Logatchev hydrothermal site (Mid-Atlantic Ridge). *J Mar Biol Assoc UK* 81:655–661.
53. Warén A, Bouchet P (2001) Gastropoda and monoplacophora from hydrothermal vents and seeps; new taxa and records. *Veliger* 44:116–231.
54. Taylor JD, Williams ST, Glover EA (2007) Evolutionary relationships of the bivalve family Thyasiridae (Mollusca: Bivalvia), monophyly and superfamily status. *J Mar Biol Assoc UK* 87:565–574.
55. Lartaud F, et al. (2010) Fossil clams from a serpentinite-hosted sedimented vent field near the active smoker complex Rainbow (MAR, 26°13'N): insight into the biogeography of vent fauna. *Geochim Geophys Geosyst* 11:Q0AE01.
56. Gebruk AV, Chevaldonné P, Shank T, Lutz RA, Vrijenhoek RC (2000) Deep-sea hydrothermal vent communities of the Logatchev area (14°45'N, Mid-Atlantic Ridge): Diverse biotopes and high biomass. *J Mar Biol Assoc UK* 80:383–393.
57. Oliver PG, Holmes AM (2006) New species of Thyasiridae (Bivalvia) from chemosynthetic communities in the Atlantic Ocean. *J Conchol* 39:175.
58. Charlou JL, Donval JP, Fouquet Y, Jean-Baptiste P, Holm N (2002) Geochemistry of high H<sub>2</sub> and CH<sub>4</sub> vent fluids issuing from ultramafic rocks at the Rainbow hydrothermal field (36°14'N, MAR). *Chem Geol* 191:345–359.
59. Childress JJ, Fisher CR, Favuzzi JA, Sanders NK (1991) Sulfide and carbon-dioxide uptake by the hydrothermal vent clam, *Calyptogena magnifica*, and its chemoautotrophic symbionts. *Physiol Zool* 64:1444–1470.
60. Früh-Green GL, Connolly JA, Plas A (2004) Serpentinization of oceanic peridotites: Implications for geochemical cycles and biological activity. *The Subsurface Biosphere at Mid-Ocean Ridges*, eds WSD Wilcock, EF DeLong, DS Kelley, JA Baross, and SC Cary (American Geophysical Union, Washington, DC), Vol 144.
61. Ildefonse B, et al. (2007) Oceanic core complexes and crustal accretion at slow-spreading ridges. *Geology* 35:623–626.
62. Hopkinson L, Beard JS, Boulter CA (2004) The hydrothermal plumbing of a serpentinite-hosted detachment: Evidence from the West Iberia non-volcanic rifted continental margin. *Mar Geol* 204:301–315.
63. Alt JC, Shanks WC (2006) Stable isotope compositions of serpentinite seamounts in the Mariana forearc: serpentinization processes, fluid sources and sulfur metasomatism. *Earth Planet Sci Lett* 242:272–285.
64. Sponheimer M, Lee-Thorp JM (1999) Isotopic evidence for the diet of an early Hominid, *Australopithecus africanus*. *Science* 283:368–370.
65. Ségalen L, Lee-Thorp JM (2009) Palaeoecology of late Early Miocene fauna in the Namib based on <sup>13</sup>C/<sup>12</sup>C and <sup>18</sup>O/<sup>16</sup>O ratios of tooth enamel and ratite eggshell carbonate. *Palaeogeogr Palaeoclimatol Palaeoecol* 277:191–198.
66. Robinson LF, Henderson GM, Slowey NC (2002) U-Th dating of marine isotope stage 7 in Bahamas slope sediments. *Earth Planet Sci Lett* 196:175–187.
67. Edwards RL, Chen JH, Wasserburg GR (1986) <sup>238</sup>U-<sup>234</sup>U-<sup>230</sup>Th-<sup>232</sup>Th systematics and the precise measurement of time over the past 500,000 years. *Earth Planet Sci Lett* 81:175–192.
68. Bayon G, Henderson GM, Bohn M (2009) U-Th stratigraphy of a cold seep carbonate crust. *Chem Geol* 260:47–56.